

BUBBLE GROWTH IN FLASH EVAPORATION

Sridhar Gopalakrishna* and Noam Lior

University of Pennsylvania, Philadelphia, PA 19104-6315
*Rutgers University, Piscataway, NJ, USA

The objective of this study is to investigate numerically the transient growth of a vapor bubble in a liquid under flash evaporation conditions, i.e. when the surrounding pressure field is decaying with time.

Results are obtained for different flash-down pressure drops, pressure decay rates, Peclet numbers, and salt concentrations. Some of the primary conclusions are: (1) the growth curves show a $t^{3/2}$ power dependence of the radius as a function of time t , (2) higher externally-imposed rates of pressure decay increase the bubble growth rates, up to three-fold in the cases considered in this study. Comparison to other researchers' experimental and theoretical results is favorable.

The primary contribution is in considering a prescribed transient driving pressure difference, and limiting cases of liquid temperature profiles, both considerations bringing flash evaporation bubble growth analysis much closer to reality than accomplished so far.

1. INTRODUCTION

The vapor generation process in flash evaporation involves the liberation of bubbles from the bulk of the liquid. These bubbles originate from existing gas nuclei or solid particles which act as sites for heterogeneous vapor nucleation in the bulk liquid. The bubbles, once generated, can grow under the influence of the existing superheat in the bulk liquid, which results from the pressure reduction in the vapor space.

The problem of spherical phase growth and collapse has captured the attention of many researchers over the last 30 years. Plesset and Zwick (1954), as well as Forster and Zuber (1954) originally solved the problem of spherical growth of a vapor bubble in an infinite liquid with uniform superheat. It has been confirmed by many experiments that bubble growth is initially controlled by surface tension, then by liquid inertia, and finally by heat transfer in the liquid. Most of the earlier studies assumed heat transfer-controlled growth because of the fact that the initial stages last for a very short time. Later extensions to the uniform superheat calculations included the addition of time-dependent superheats, mass diffusion of noncondensables, and nonequilibrium at the bubble interface among other fac-

tors (cf. Mikic, Rohsenow and Griffith (1970), Zwick (1960), Jones and Zuber (1976), Buelbach and Bankoff (1987), Toda and Kitamura (1983), Cha and Henry (1982), Theofanous et al. (1969), Inoue and Aoki (1975), Wittke and Chao (1967), Ruckenstein and Davis (1971), Pinto and Davis (1971)). Darby (1964) examined experimentally nucleate boiling from a heated surface enclosing a pool of liquid. Hooper et al. (1966) studied the flashing phenomenon by suddenly reducing the pressure in the vapor space above a pool of liquid, with superheats of up to 36°C . Abdelmessih (1968) considered spherical bubble growth in a highly superheated liquid. Based on the experiments of Hooper et al. described above, he developed a correlation for the radius as a quadratic function of the imposed superheat. The commonly used expression ($t^{1/2}$ relationship) was shown to deviate from the experimental results for cases when the superheats are high (of the order of 25°C).

The objectives of this analysis are: a) to solve for the temperature field around a vapor bubble for a low Reynolds number flow caused by bubble growth and translation in an infinite volume of liquid, and b) to predict the bubble growth history for a vapor bubble for various translation velocities in a pressure field which corresponds to that found in flashing.

2. PROBLEM FORMULATION

The following assumptions are made to simplify the problem: (1) Spherical bubble. For typical conditions, the Weber number is in the range of 0.1, which would keep the bubble spherical, (2) Rectilinear bubble motion in the vertical direction, (3) Infinite expanse of the liquid for the time period of bubble motion, (4) Constant surface tension, (5) Uniform temperature and pressure inside the growing bubble, (6) Local equilibrium conditions at the interface, (7) Growth of the bubble limited by heat transfer in the liquid, (8) Constant translation velocity corresponding to a range from creeping flow to potential flow ($0 < Re < 50$) for the range of parameters considered, (9) Bubble nucleation at a certain depth has already occurred by means of heterogeneous nucleation on preferred sites within the liquid, and the initial conditions for growth are thus specified. The temperature differences driving bubble growth in the range of parameters considered here are of the order of a few degrees C, and the pressure differences are correspondingly small. As lim-

iting cases, we examine a step increase in the superheat which causes the bubble to grow as a result of the sudden pressure drop in the vapor space above the liquid, and also a linearly increasing temperature profile extending from the bubble surface temperature to the value far away from the bubble in the liquid. In a realistic case, where many bubbles grow simultaneously, the temperature of the liquid between adjacent bubbles rises from the interface of one bubble to the liquid mid-point between the bubbles, and then decreases to the interface of the second bubble. A linear temperature profile is one simple limiting case representing this situation, (10) Mass diffusion is not considered as an additional transport process. Its influence was estimated using an order of magnitude analysis for typical concentrations of dissolved air in water, and was found to be small.

The schematic of the problem is shown in Fig. 1. The origin is taken to be the center of the bubble and moving with it. Spherical polar coordinates are employed for the problem description. Azimuthal symmetry renders the problem two-dimensional (r, θ).

The flow problem involves the simultaneous solution of the momentum balances on either side of the moving bubble interface. Such a solution of the equations of motion for the case of creeping motion (that is, when the inertial terms are negligible) has been derived by Hadamard and Rybczynski. For a bubble of radius R traveling at velocity U_∞ , their solution can be expressed in terms of the stream function ψ :

$$\psi_l = -U_\infty \frac{r^2 \sin^2 \theta}{2} \left[1 - \frac{(2 + 3\kappa)R}{2(1 + \kappa)r} + \frac{\kappa}{2(1 + \kappa)} \frac{R^3}{r^3} \right], \quad (1)$$

$$\psi_v = U_\infty \frac{r^2 \sin^2 \theta}{4(1 + \kappa)} \left[1 - \frac{r^2}{R^2} \right] \quad (2)$$

This flow solution is next employed in the thermal energy equation for the liquid phase. For a growing bubble, a superimposed radial velocity representing the growth rate is also considered. The liquid energy equation is written as:

$$\frac{\partial T}{\partial t} + u_r \frac{\partial T}{\partial r} + \frac{u_\theta}{r} \frac{\partial T}{\partial \theta} = \alpha \nabla^2 T, \quad r > R \quad (3)$$

The energy balance at the interface gives:

$$\frac{d}{dt} \left(\frac{4}{3} \pi R^3 \rho_v h_{fg} \right) = - \int_0^\pi k \frac{\partial T}{\partial r} (R, \theta, t) 2\pi R^2 \sin \theta d\theta \quad (4)$$

The following limiting cases of initial temperature conditions are used:

Linear Temperature Profile:

$$T(r, \theta, 0) = T_{sat,0} + (T_\infty - T_{sat,0}) \left(\frac{r}{R_{ref}} \right). \quad (5)$$

Step Temperature Profile:

$$\begin{aligned} T(r, \theta, 0) &= T_\infty, & r > R_0 \\ T(r, \theta, 0) &= T_{sat,0}, & r = R_0 \\ T(R, \theta, t) &= T_{sat} & \text{at } r = R \\ T(\infty, \theta, t) &= T_\infty \end{aligned} \quad (6)$$

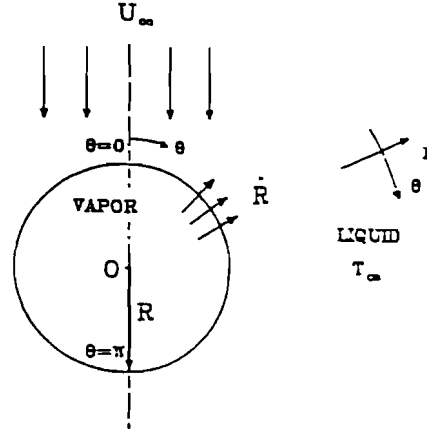


Figure 1: Schematic of Bubble Growth and Motion during Flashing

where R_{ref} is an arbitrary reference radius (far away from the bubble interface).

For an assumed exponential decay of the vapor space pressure reduction (this has been shown to be a valid model by Kung and Lester 1981), the pressure p in the vapor space at any time can be written as:

$$p = p_f + (p_i - p_f)e^{-\beta t} = p_i (p^* + (1 - p^*)e^{-\beta t}) \quad (7)$$

where p_i is the initial and p_f the final vapor space pressures, and β is the inverse of the time constant of the depressurization transient. Clapeyron's equation:

$$\frac{1}{T(0)} - \frac{1}{T(R, \theta, t)} = \frac{\tilde{R}}{h_{fg}} \ln \frac{p}{p_i} \quad (8)$$

This relation can be used to relate the bubble surface temperature to the given pressure reduction characteristics.

2.1 Scaling

The following dimensionless quantities are introduced:

$$\tau = \frac{\alpha t}{R_0^2}, \quad \gamma = \frac{R}{R_0}, \quad y = \frac{r - R}{R_0}, \quad \bar{u} = \frac{u}{U_\infty}, \quad \Theta = \frac{T - T_\infty}{T_{sat,0} - T_\infty} \quad (9)$$

A further transformation in the radial coordinate is employed as follows:

$$y = e^z - 1$$

This results in finer grid spacing near the bubble surface and coarser spacing far away from the surface.

Using equations (1) and (2) for the velocities and equations (9) for scaling in equation (3), we get:

$$\begin{aligned} \frac{\partial \Theta}{\partial \tau} + \left\{ \left(\frac{\tau}{y + \gamma} \right)^2 \frac{d\tau}{d\tau} - \frac{d\tau}{d\tau} - \frac{Pe}{2} \cos \theta \left[1 + K_1 \left(\frac{\tau}{y + \gamma} \right) - K_2 \left(\frac{\tau}{y + \gamma} \right)^2 \right] \right\} \frac{\partial \Theta}{\partial y} \\ + \frac{Pe \sin \theta}{2} \frac{1}{(y + \gamma)} \left[1 - \frac{K_1}{2} \left(\frac{\tau}{y + \gamma} \right) - \frac{K_2}{2} \left(\frac{\tau}{y + \gamma} \right)^2 \right] \frac{\partial \Theta}{\partial \theta} \\ = \frac{\partial^2 \Theta}{\partial y^2} + \frac{2}{(y + \gamma)} \frac{\partial \Theta}{\partial y} - \frac{1}{(y + \gamma)^2} \frac{\partial^2 \Theta}{\partial \theta^2} + \frac{\cot \theta}{(y + \gamma)^2} \frac{\partial \Theta}{\partial \theta} \end{aligned} \quad (10)$$

where Pe is the Peclet Number ($= U_\infty R/\alpha$). Note that the translation velocity U_∞ is used as the velocity scale in the calculation of Peclet Number. The growth term is represented by $\frac{dr}{dt}$. For a growing and translating bubble, the natural velocity scale is the velocity of translation.

The growth rate equation now becomes:

$$\dot{r} = \frac{Ja}{2} \int_0^\pi \frac{\partial \Theta}{\partial y}(0, \theta, t) \sin \theta d\theta, \quad \gamma(0) = 1 \quad (11)$$

In the above equation, Ja represents the Jakob Number signifying the effect of liquid superheat on bubble growth. The set of equations (10) and (11), with the conditions in dimensionless form constitute a complete set for the determination of γ as a function of time for given parameter values Ja (equivalently, by a specification of the pressure reduction parameters in equation (7) and Pe). The results obtained are limited to spherical bubbles (as determined by the limiting Weber Number) and also to situations where bubble spacing is such that bubble coalescence is not an important mechanism. The range of radii examined here is still relevant to a typical flash evaporation situation where many bubbles form and coalesce for large radius ratios.

3. SOLUTION PROCEDURE

Equations (10) and (11) are solved numerically using the finite difference Alternating Direction Implicit (ADI) method.

During the numerical integration, checks are made in the program to ensure convergence. The radial step increments in the numerical scheme are taken such that the change in the computed temperature far away from the bubble surface compared to the value at infinity is less than a prescribed tolerance limit (typically 10^{-3} corresponding to $0.01^\circ C$ for $T_0 = 100^\circ C$). The calculations are terminated when the Weber number reaches a level of about 0.1 (the assumption of spherical shape being questionable at this stage). The thermodynamic properties are taken to be functions of temperature.

Table 1 gives a list of the ranges of parameters and dimensional quantities that correspond to the calculations.

Quantity	Typical value
Temperature, $T_0, ^\circ C$	100
Radius, R , mm	0.1
Rise Velocity, U_∞ , m/s	0.2
Peclet Number, Pe	100
Jakob Number, Ja	50
Reynolds Number, Re	20
Salinity, C , %	3.5
Prandtl Number, Pr	2.14
Weber Number, We	0.05
Time constant, β^{-1} , ms	100
β , s^{-1}	10
p^*	0.5

Table 1: Parameters and Physical Variables used in the Numerical Solution of Bubble Growth

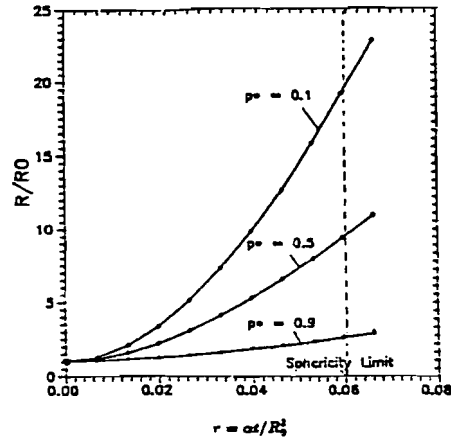


Figure 2: Bubble Growth as a Function of Time for Different p^* and Pe ; $\beta = 20 s^{-1}$, Linear Initial Temperature Profile. The Three Curves Corresponding to $Pe = 0, 10$ and 100 for each p^* Merge into One Line

4. RESULTS AND DISCUSSION

The results are primarily expressed in the form of growth curves.

As described in the problem formulation, the cause of local superheat in the liquid which causes the bubble to grow is the reduction of pressure in the vapor space above the liquid. Therefore, the primary parameters which control the entire transient are the magnitude and rate of this pressure reduction, quantified by $p^*(= p_f/p_i)$ and β . Translation of the bubble is represented by the Peclet number (Pe), and C is the salinity of the liquid. The range of parameters chosen covers a range of engineering interest for flash evaporation. All the illustrations employ a dimensionless time defined by $r = \alpha t/R_0^2$, and the type of initially imposed temperature profile is also indicated.

Figure 2 shows the dimensionless bubble radius as a function of time up to about 0.1 seconds. As shown by the three different pressure reductions, a larger pressure reduction (corresponding to $p^* = 0.1$) results in a steeper growth curve as compared to a smaller reduction ($p^* = 0.9$). The available superheat for bubble growth is higher for the larger pressure drop, and this results in increased driving forces for growth. The dimensionless bubble radius reached for the case of $p^* = 0.1$ at larger times, shows that an order of magnitude difference can occur in the bubble size if the imposed pressure reduction is large enough. An important feature in Fig. 2 is the change of the radius as a function of time. The conventional asymptotic solution (for bubble growth governed by heat transfer in the liquid alone) predicts a $t^{1/2}$ dependence. However, a $t^{3/2}$ dependence is observed in this study, because this case addresses a nonuniform temperature field, in contrast to the uniform levels of superheat examined by most researchers. The trend shown here follows the one given by Zwick (1960) for the case of a rapidly heated liquid, and the comparison with that study is made further below.

Figure 3 shows the effect of changing the translation Peclet number on the growth curve. The curves in this figure have

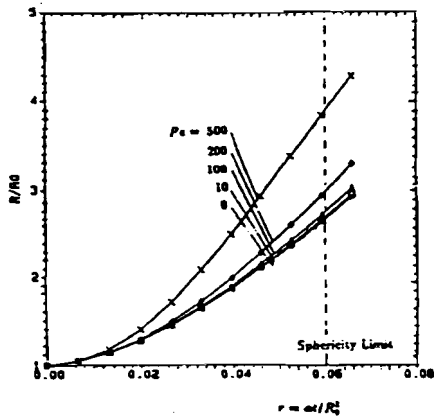


Figure 3: Effect of Translation Peclet Number on Bubble Growth; $p^* = 0.9$, $\beta = 20 \text{ s}^{-1}$, Linear Initial Temperature Profile

also been drawn for Peclet numbers beyond the range of Table 1, in order to illustrate the trend. The creeping flow solutions are strictly valid only up to $Pe \approx 1$. Although Pe is very high for some of the calculations, those calculations were done for extrapolation purposes, to examine trends only. Translation is seen to increase the growth, but only slightly for the range considered in this study, i.e. $0 \leq Pe \leq 100$. The relative contributions of the growth and translation terms in equation (10) are different for the different cases of pressure reductions considered here. For low pressure reductions (high p^*), the bubble translation term causes convection of heat along the bubble translation axis (in the infinite expanse of liquid assumed in this study) and therefore the local superheat is sustained at a high level since the bubble in its motion, becomes exposed to fresh liquid, thus increasing the growth rate. On the other hand, as seen in Fig. 4, the Peclet number does not have any perceptible effect for high pressure reduction (low p^*). The growth term in equation (10) overcomes the contribution from the translation term sufficiently, and the radial latent heat transfer from the liquid to the vapor controls the resulting growth behavior. It may be noted from the Figure 3 that a Pe of 500 results in almost 50 % higher radius than that at a Pe of 100 after about 0.1 seconds.

Figure 5 shows that the growth rate is higher for the initial step profile, because of the availability of high local superheat. For later times, this immediate effect will be reduced as the temperature profile becomes flatter, and the initial profile is not likely to have a significant effect.

Figure 6 shows the effect of varying the time constant of pressure reduction on the growth curve. By changing the parameter β in the pressure reduction equation (7), a range of pressure drops—from a 'step' reduction to a 'smooth' reduction can be simulated. The lowest curve in the figure corresponds to a very slow reduction, where the pressure remains practically at the initial value. As expected, the growth is slowest for this case (the nonzero growth occurs due to conduction in the

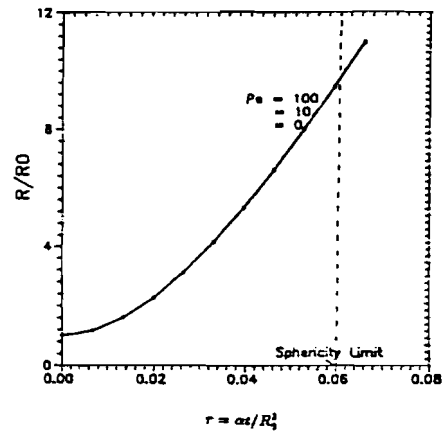


Figure 4: Effect of Translation Peclet Number on Bubble Growth; $p^* = 0.1$, $\beta = 20 \text{ s}^{-1}$, Linear Initial Temperature Profile

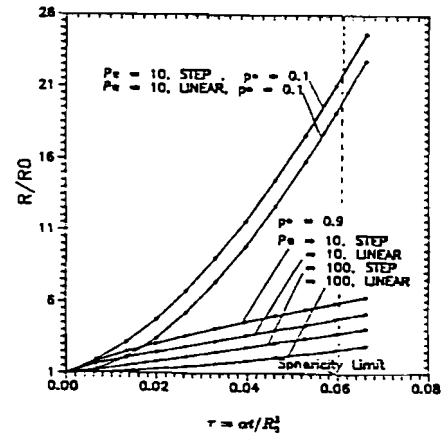


Figure 5: Effect of the Initial Temperature Field Around the Bubble on Growth; $Pe = 10$, $\beta = 20 \text{ s}^{-1}$. 'STEP' Represents an Initial Step Temperature Profile Starting from the Bubble Wall to a Region far away from the Bubble. 'LINEAR' Corresponds to a Linearly Varying Profile

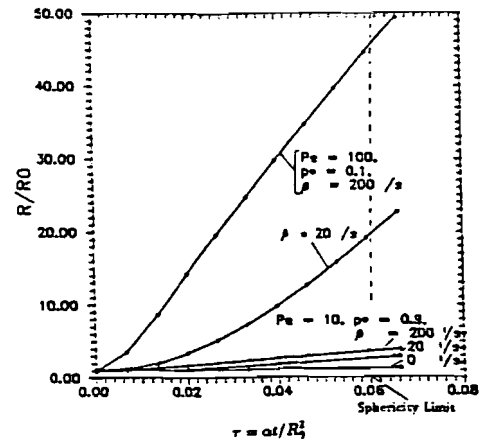


Figure 6: Effect of the Time Constant of the Pressure Reduction on Bubble Growth, Linear Initial Temperature Profile

liquid). The imposition of a sudden pressure reduction (corresponding to a time constant of 5 milliseconds) results in the highest growth curve. However, as time goes on, the growth rate is not increasing, and even decreases slightly, in contrast with the lower curves which still show an increase in the growth rate.

Figure 7 shows the effect of salinity of the liquid pool as a parameter in the calculation of thermophysical and transport properties of the liquid. A complete analysis would include the mass diffusion equation for salt. However, for the short-time, heat transfer-controlled growth considered here, that diffusion has a small effect, and boiling point elevation is probably the dominant (although not sole) effect of salinity on bubble growth. Two values of the salt concentration were examined here: 0, for pure water, and 0.035 for water with 3.5% concentration of salt (typical sea water, used in desalination where flash evaporation distillation is widely used). Since the flashing occurs due to the imposition of pressure reduction in the vapor space, this pressure ratio is the governing parameter in the resulting process, and thus the effect of salinity was examined here via the elevation of the boiling point. In the numerical code, the boiling point elevation corresponding to the concentration of the salt in the solution is computed using a correlation developed by Fabuss and Korosi, as a function of temperature, pressure and concentration. This additional temperature rise is used in equation (8) for the saturation temperature.

Figure 7 shows that bubbles grow faster for the higher salinity cases. Indeed, the direct increase of the available superheat close to the bubble wall, due to the boiling point elevation, results in increased growth. Since the level of local temperature elevation caused by salinity is of the order of 0.5°C , this effect is important at the lower pressure reductions.

Zwick's model (1960) is more representative of the conditions under investigation in this study, and the slope of the growth curve is indeed less steep in the early stages and increases with time. Figure 8 compares our results with those available in the literature on bubble growth in flashing. The data of Abdelmessih (1968) for high superheats, and the data of Miyatake et al. (1980) - both for uniform superheats - are used for comparison. The comparison is shown because these experimental data are the only ones available in our range of interest, and it does demonstrate similar overall values (although not necessarily trends, because of the different conditions). Those results show a typical $t^{1/2}$ profile for radius as a function of time. However, the comparison of the growth curve from our computations (for creeping flow conditions and for $We < 0.1$) is in excellent agreement with a $t^{3/2}$ profile, as found by Zwick (1960). The nonuniform superheats encountered here are an essential feature of the process, as shown by the comparison with Zwick's data.

5. CONCLUSIONS

(1) Bubble growth is proportional to $t^{3/2}$, as found by Zwick (1960) for the case of a varying superheat surrounding the bubble.

This behavior of the bubble radius as a function of time is in direct contrast to that for a uniform superheat (Plesset and Zwick, 1954, and Forster and Zuber, 1954) where a $t^{1/2}$ dependence on time is observed.

(2) Translation increases the size of the bubble for low superheats. For large Peclet numbers, the effect can be up to 50%.

(3) Bubble growth rates increase with the initial temperature gradient in the liquid at the bubble interface.

(4) Bubble growth rates increase with the rate of vapor space pressure reduction.

(5) Bubble growth rates increase with salinity, especially for small pressure reductions.

6. ACKNOWLEDGEMENT

This work was supported in part by a grant from DOE, Office of Conservation and Renewable Energy. We would like to thank the International Desalination Association for the award of a one-year scholarship to one of the authors (SG). Professor O. Miyatake provided many valuable discussions throughout this work.

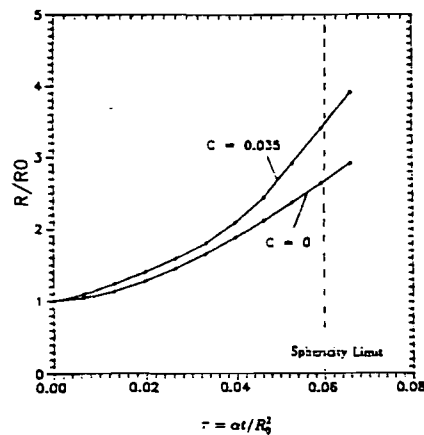


Figure 7: Effect of Salinity of the Pool on Bubble Growth: $p^* = 0.9$, $Pe = 10$, $\beta = 20 \text{ s}^{-1}$, Linear Initial Temperature Profile

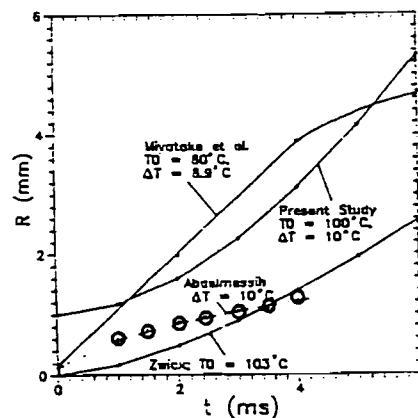


Figure 8: Comparison with Miyatake et al. (1987), Abdelmessih (1968), Zwick (1960); $p^* = 0.9$, $Pe = 0$, $\beta = 20 \text{ s}^{-1}$, Linear Initial Temperature Profile

6. NOMENCLATURE

C_D	drag coefficient
C_p	specific heat of the liquid
C	concentration of NaCl in the solution
h_{fg}	latent heat of vaporization
Ja	Jakob number, $\Delta T C_p / h_{fg}$
k	thermal conductivity of liquid
p_f	final pressure in the vapor space
p_i	initial vapor space pressure
Pe	Peclet number, $2U_\infty R_0 / \alpha_l$
Pr	Prandtl number, $C_p \mu / k$
r	radial coordinate
R	bubble radius at any time t
R_0	initial radius of the bubble
Re	Reynolds number, $2RU_\infty / \nu_l$
t	time
t_d	traversal time for the pressure wave
T_0	initial temperature of the pool
T_{sat}	saturation temperature inside the bubble
T_∞	liquid temperature far away from the bubble
T_w	bubble surface temperature
U_∞	liquid velocity far from the bubble
We	Weber number, $2RU_\infty^2 \rho_l / \sigma$
α	thermal diffusivity
β	time constant of the depressurization
γ	dimensionless radial coordinate
θ	angular coordinate
Θ	dimensionless temperature
κ	ratio of viscosities μ_v / μ_l
μ	viscosity
ρ	density
σ	surface tension
τ	dimensionless time
ψ	stream function
Δp	pressure drop in the vapor space
ΔT	superheat in the liquid

7. REFERENCES

- Abdelmessih, A. H. "Spherical Bubble Growth in a Highly Superheated Liquid Pool", Int. Symp. on Research in Concurrent Gas-Liquid Flow, University of Waterloo, Waterloo, Canada, Preprints 9.18 - 9.19, 1968.
- Burelbach, J. P. and Bankoff, S. G. "Vapor Bubble Growth under Decompression Conditions", *PhysicoChemical Hydrodynamics*, Vol. 9, No. 1/2, pp. 15-22, 1987.
- Cha, Y. S. and Henry, R. E. "Bubble Growth During Decompression of a Liquid", *J. Heat Transfer*, Vol. 103, pp. 56-60, 1981.
- Clift, R., Grace, J. R. and Weber, M. E. *Bubbles, Drops and Particles*, Academic Press, 1978.
- Darby, R. "The Dynamics of Vapor Bubbles in Nucleate Boiling", *Chem. Eng. Sci.*, Vol. 19, pp. 39-49, 1964.
- Forster, H. K. and Zuber, N. "Growth of a Vapor Bubble in a Superheated Liquid", *J. Applied Physics*, Vol. 25, No. 4, pp. 474-478, 1954.
- Gopalakrishna, S. "Studies on Enclosed Pool Flash Evaporation", Ph.D. Thesis, University of Pennsylvania, Philadelphia, 1989.
- Hooper, F. C. and Kerba, N. A. "A Law of Flashing", 3rd Int. Heat Transfer Conference, Paper No. 117, 1966.
- Inoue, A. and Aoki, S. "On the Dynamics of Bubble Growth under Time - Dependent Pressure Field", *Bulletin of the Tokyo Institute of Technology*, No. 127, pp. 25-43, 1975.
- Jones, O. C. Jr. and Zuber, N. "Evaporation in Variable Pressure Fields", CSME Paper No. 76-CSME/CSCHE-12, 1976.
- Kung, S. P. and Lester, T. W. "Boiling Transition During Rapid Decompression From Elevated Pressures", ASME Paper 81-WA/HT-57, 1981.
- Mikic, B. B., Rohsenow, W. M. and Griffith, P. "On Bubble Growth Rates", *Int. J. Heat Mass Transfer*, Vol. 13, pp. 657-666, 1970.
- Miyatake, O. and Tanaka, I. "Numerical Analysis of Bubble Growth in Uniformly Superheated Water at Reduced Pressures", Research Report, Kyushu University, Vol. 71, pp. 13-28, 1980.
- Pinto, Y. and Davis, E. J. "The Motion of Vapor Bubbles Growing in Uniformly Superheated Liquids", *AIChE Journal*, Vol. 17, No. 6, pp. 1452-1458, 1971.
- Plesset, M. S. and Zwick, S. A. "The Growth of Vapor Bubbles in Superheated Liquids", *J. Applied Physics*, Vol. 25, pp. 493-500, 1954.
- Ruckenstein, E. and Davis, E. J. "The Effects of Bubble Translation on Vapor Bubble Growth in a Superheated Liquid", *Int. J. Heat Mass Transfer*, Vol. 14, pp. 939-952, 1971.
- Theofanous, T., Biasi, L., Isbin, H. S. and Fauske, H. "A Theoretical Study on Bubble Growth in Constant and Time-Dependent Pressure Fields", *Chem. Eng. Sci.*, Vol. 24, pp. 885-897, 1969.
- Toda, S. and Kitamura, M. "Bubble Growth in Decompression Fields", ASME/JSME Thermal Engineering Conference, Vol. 3, pp. 395-402, 1983.
- Wittke, D. D. and Chao, B. T. "Collapse of Vapor Bubbles with Translatory Motion", *J. Heat Transfer*, Vol. 89, pp. 17-24, 1967.
- Zwick, S. A. "Growth of Vapor Bubbles in a Rapidly Heated Liquid", *Physics of Fluids*, Vol. 3, No. 5, pp. 685-692, 1960.